Eur. Phys. J. Special Topics **226**, 1287–1296

DOI: 10.1140/epjst/e2016-60228-8

THE EUROPEAN PHYSICAL JOURNAL
SPECIAL TOPICS

Regular Article

Parametric excitation of oscillatory Marangoni instability in a heated liquid layer covered by insoluble surfactant

Alexander B. Mikishev[1,2,a] and Alexander A. Nepomnyashchy[3,b]

[1] Department of Physics, Sam Houston State University, Huntsville, TX 77341, USA
[2] Embry-Riddle Aeronautical University-Worldwide, Daytona Beach, FL 33114, USA
[3] Department of Mathematics, Technion - Israel Institute of Technology, Haifa 32000, Israel

Received 15 July 2016 / Received in final form 5 August 2016
Published online 2 May 2017

Abstract. This paper is a continuation of our previous research reported in the two last IMA conferences. While in our previous works the driving modulation was a modulation of the temperature gradient, here the temperature gradient is fixed in the whole liquid layer and the liquid is vertically vibrated with some fixed driving frequency. Two kinds of waves can be generated in this system. The first kind of waves are transverse (capillary-gravity) waves. The second kind of waves are longitudinal (Marangoni) waves caused by the dependence of the surface tension on the temperature and the surfactant concentration. A linear analysis with arbitrary wave numbers is performed. Two different heating regimes were considered. Multiple instability regions depending on the heating conditions are analyzed. Among three possible modes of the system's response to external forcing, the most "dangerous" one is the subharmonic instability mode.

1 Introduction

It is well known that the influence of external parametric excitation on a physical system can change the behavior of this system. Faraday was a pioneer who documented the parametric resonance, observing capillary-gravity waves with frequency of half the driving frequency in a fluid-filled container under vertical vibrations [1]. Later, Melde [2] was the scientist who first observed the phenomenon of parametric resonance in structural mechanics, finding that a string could oscillate laterally although the driving force was longitudinal. Only in two decades Lord Rayleigh (J.W. Strutt) [3] theoretically interpreted these phenomena and his analysis led to new experiments with other physical systems (for example, electrical circuits [4]). The quantitative theory of the Faraday instability has been developed by Benjamin and

[a] e-mail: amik@shsu.edu
[b] e-mail: nepom@technion.ac.il

Ursell [5] in the case of an ideal liquid and by Kumar [6] in the case of a viscous liquid.

Historically, the hydrodynamic systems under parametric excitation are the ones most extensively studied [7–9]. Depending on the amplitude and frequency of the driving force, the instability thresholds as well as the nonlinear dynamics of the convective systems are modified.

Here we continue to consider the hydrodynamic systems represented by the horizontal liquid layer heated from below or above and with the upper free surface of this liquid volume covered by insoluble surfactant. The system described above is subject to two kinds of oscillatory motions, (i) transverse waves (deformations of the surface) caused by a joint action of gravity and surface tension, and (ii) longitudinal waves (redistributions of temperature and surfactant concentration along the surface) driven by the gradient of the surface tension. Normally, both kinds of waves decay due to dissipative effects. However, by heating from above, mode mixing can create an instability which manifests itself as a spontaneous excitation of a definite mixed mode (for details, see [10–12]). By heating from below, the advection of the surfactant by the liquid motion creates a surface tension inhomogeneity, which generates tangential stresses directed opposite to the liquid motion. That circumstance can lead to a longitudinal oscillatory instability [13–15].

In the present paper we consider the parametric excitation of this system by shaking the liquid volume vertically up and down with a given driving frequency. The applied driving mechanism is not crucial, thus with some level of abstraction we can say that this work is a continuation of our previous works, where the driving mechanism is the modulation of temperature gradient [16,17]. Because our main point of investigation is processes near the surface, we consider a semi-infinite liquid layer. Section 2 contains the formulation of the problem. Section 3 briefly describes the applied numerical method. Computation results are presented in Section 3. Section 4 consists of conclusions.

2 Formulation of the problem

2.1 Basic equations and boundary conditions

We consider a semi-infinite volume of an incompressible Newtonian liquid with free upper deformable boundary $z = \zeta(x,t)$. The undisturbed surface is located at $z = 0$, and the bottom of the volume approaches negative infinity, $z \to -\infty$ (the z-axis is directed vertically upward). The liquid volume is subjected to vertical harmonic vibrations $a\cos(2\Omega t)$, as well as to a transverse temperature gradient, $-A$, maintained throughout the liquid. The thermal gradient is directed downward, $A > 0$, for heating from below and directed upward, $A < 0$, for heating from above. Here a is the amplitude of the external vibrations, 2Ω is the external modulation frequency, and t is time. The upper surface of the liquid volume is covered by insoluble surfactant with concentration $\Gamma(x,t)$. For a linear analysis of the problem the consideration of a two-dimensional problem is relevant. The scheme of the problem is depicted in Figure 1.

On the disturbed upper surface $z = \zeta(x,t)$ the evolution of the surfactant concentration $\Gamma(x,t)$ is governed by the equation

$$\Gamma_t - \zeta_t(\mathbf{e}_z \cdot \nabla_s)\Gamma + \nabla_s \cdot (\mathbf{v}_\tau \Gamma) + (\nabla_s \cdot \mathbf{n})(\mathbf{v} \cdot \mathbf{n})\Gamma = D\nabla_s^2\Gamma, \tag{1}$$

see [18]. Here $\mathbf{v} = (u, 0, w)$ is the velocity field, $\nabla_s = \nabla - \mathbf{n}(\mathbf{n} \cdot \nabla)$, $\nabla = (\partial_x, \partial_z)$, $\mathbf{n} = (-\zeta_x, 1)(1 + \zeta_x^2)^{-1/2}$ is the unit vector normal to the interface, $\mathbf{v}_\tau = \mathbf{v} - (\mathbf{v} \cdot \mathbf{n})\mathbf{n}$ is the

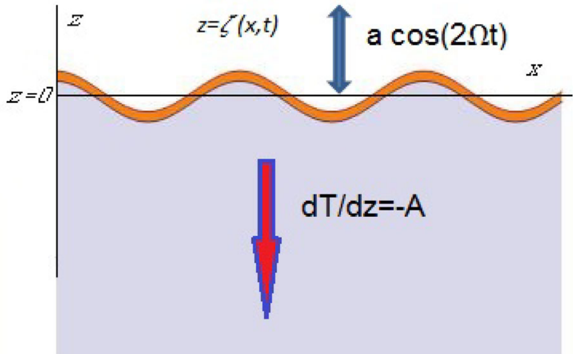

Fig. 1. Scheme of the problem.

tangential component of velocity, D is the surface diffusion coefficient, and $\mathbf{e}_z = (0, 1)$ is a unit vector directed upwards. The subscript denotes the partial derivative with respect to the corresponding variable.

On the upper free surface the standard Newton's cooling law is applicable

$$\lambda \partial_{\mathbf{n}} T + q(T - T_g) = 0, \tag{2}$$

where λ is the thermal conductivity of the fluid, q is the rate of the heat transfer by convection at the free surface, and T_g is the bulk temperature of the gas above the liquid layer. The surface tension linearly depends on the deviations of the temperature and the surfactant concentration from their reference values:

$$\sigma = \sigma_0 - \sigma_1(T - T_0) - \sigma_2(\Gamma - \Gamma_0). \tag{3}$$

Here $\sigma_1 = -\partial_T \sigma > 0$, $\sigma_2 = -\partial_\Gamma \sigma > 0$, σ_0, T_0, and Γ_0 are, respectively, the reference values of surface tension, temperature and the surfactant concentration.

The process in the liquid is governed by the following equations of momentum, mass and energy conservation

$$\mathbf{v}_t + (\mathbf{v} \cdot \nabla)\mathbf{v} = -\rho^{-1}\nabla p + \nu \nabla^2 \mathbf{v} + \mathbf{g} - 4a\Omega^2 \cos(2\Omega t)\mathbf{e_z}, \tag{4}$$

$$\nabla \cdot \mathbf{v} = 0, \tag{5}$$

$$T_t + (\mathbf{v} \cdot \nabla)T = \chi \nabla^2 T, \tag{6}$$

where ρ, ν, and χ are density, kinematic viscosity, and thermal diffusivity, respectively.

To complete the formulation of the problem we add to conditions (1)–(3) the balance conditions for the normal and tangential stresses on the upper free surface as well as the kinematic condition,

$$z = \zeta(x, t) : -p + 2\mu \mathbf{n} \cdot \mathcal{D} \cdot \mathbf{n} + 2H\sigma = 0, \tag{7}$$

$$2\mu \mathbf{n} \cdot \mathcal{D} \cdot \mathbf{t} = \nabla \sigma \cdot \mathbf{t}, \tag{8}$$

$$\zeta_t + u\zeta_x = w, \tag{9}$$

where $\mu = \nu\rho$ is dynamic viscosity, $\mathcal{D}$ is the deviatoric stress tensor, H is the mean interfacial curvature. Here we disregard the dilational and shear viscosities of the surface.

Disturbances are located near the upper free surface and decay downwards, while the temperature gradient is retained, i.e.

$$u, w \to 0; \quad T_z \to -A \qquad \text{at} \quad z \to -\infty. \tag{10}$$

The reference solution corresponding to the quiescent state of the fluid is

$$u_b = w_b = 0, \quad \zeta_b = 0, \quad \Gamma_b = \Gamma_0, \quad p_b = -\rho g(1 - b\cos(2\Omega t))z, \quad T_b = -Az + T_{00}. \tag{11}$$

Here $b = 4a\Omega^2/g$, T_{00} is a constant unimportant for the analysis.

2.2 Nondimensional system for perturbations

Before performing the analysis of system (1)–(10) we rescale it. Here we introduce the following scales: the capillary length, $l_c = (\sigma/\rho g)^{1/2}$, is taken as a length scale, l_c^2/χ is a time scale, χ/l_c is a velocity scale, $\mu\chi/l_c^2$ is a pressure scale, Al_c is a temperature scale, and Γ_0 is a scale of the surfactant concentration.

Rewriting the system (1)–(10) in dimensionless form, we obtain a system of equations containing the following dimensionless parameters: $P = \nu/\chi$ is the Prandtl number, $L = D/\chi$ is the Lewis number, $B = ql_c/\lambda$ is the Biot number, $M = \sigma_1 Al_c^2/\mu\chi$ is the Marangoni number, $N = \sigma_2\Gamma_0 l_c/\mu\nu$ is the elasticity number, $G = gl_c^3/\nu\chi$ is the Galileo number, $F = 4a\Omega^2/g$ is the ratio between the forced acceleration and gravity acceleration, and $\omega = \Omega l_c^2/\chi$ is the dimensionless vibration frequency.

Eliminating the pressure and the horizontal component of velocity field from the linearized system of governing equations near the reference solution and introducing normal perturbations of the form

$$f(x, z, t) = \hat{f}(z, t)\exp(ikx + \Lambda t),$$

where f is any variable (vertical component of velocity, w, temperature, θ, deviation of the upper surface from the undisturbed position, ζ, surfactant concentration, γ), k and Λ are the dimensionless wave number and the growth rate of disturbances, we obtain the final set of equations with boundary conditions (later on the hats are omitted):

$$P^{-1}(w_{zzt} + \Lambda w_{zz} - k^2 w_t - \Lambda k^2 w) = w_{zzzz} - 2k^2 w_{zz} + k^4 w, \tag{12}$$

$$\theta_t + \Lambda\theta = \theta_{zz} - k^2\theta + w, \tag{13}$$

$$z = 0: \qquad \zeta_t + \Lambda\zeta = w, \tag{14}$$

$$\theta_z + B\theta = 0, \tag{15}$$

$$\gamma_t + \Lambda\gamma - w_z = -k^2 N\gamma, \tag{16}$$

$$w_{zz} + k^2 w = -Mk^2(\theta - \zeta) - k^2 N\gamma, \tag{17}$$

$$P^{-1}(w_{zt} + \Lambda w_z) + 3k^2 w_z - w_{zzz} + Gk^2(1 + k^2 - F\cos(2\omega t))\zeta = 0, \tag{18}$$

$$z \to -\infty \qquad w, w_z, \theta \to 0. \tag{19}$$

The computations presented below have been carried out in the limit $B \ll 1$, which is typically satisfied due to the low heat conductivity of the air compared to that of the liquid. Let us emphasize that the condition $B \ll 1$ does not mean that the liquid layer is thermally isolated: according to (2), the heat flux at the interface is maintained by the correspondent temperature difference between the liquid surface and the bulk of the gas. The amplitudes of variables are periodic in time functions with period π/ω.

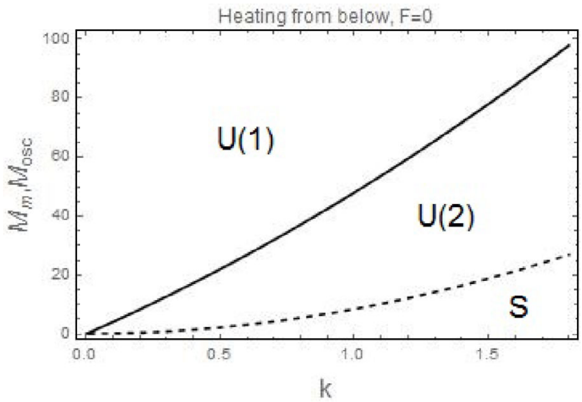

Fig. 2. Typical neutral curves. Solid line is for monotonic mode, the dashed line is for oscillatory mode. Parameters: $N = 0.1,\ L = 0.01,\ G = 100,\ P = 10,\ F = 0$. There are two eigenvalues with $Re\Lambda > 0$ in $U(2)$ and one such eigenvalue in $U(1)$. Letter "S" indicates a stable region.

3 Results

3.1 Oscillatory instabilities without parametric excitation

The system (12)–(19) without external parametric excitation ($F = 0$) has been analyzed in detail in our recent work [19]. Here we present some results of that work.

Analysis of the dispersion relation of the system (12)–(19) without external forcing ($F = 0$) was performed for two different regimes of heating: heating from below and heating from above. In the case when the liquid is heated from below ($M > 0$) we have both monotonic and oscillatory instabilities. The threshold for the monotonic instability boundary can be calculated by the formula

$$M_m = 8k^2 + 4Nk/L. \tag{20}$$

The threshold of oscillatory instability can be calculated numerically. Figure 2 shows typical neutral curves. The solid line is for the monotonic mode, the dashed line is for the oscillatory mode. For the oscillatory mode, we find that the critical Marangoni number $M = O(k)$ and the frequency $\Omega = O(k^2)$ in the longwave limit, $k \ll 1$. The full longwave dispersion relation is obtained in [19]. Here we present only the asymptotics in the limit $L \to 0$ and $P \to 1$:

$$M_{osc} = 2(1+\sqrt{3})Nk + o(k), \quad \Omega_0 = \frac{(1+\sqrt{3})3^{1/4}}{\sqrt{2}}k^2 + o(k^2). \tag{21}$$

Expressions (21) do not include the Galileo number, because the oscillatory mode generated in the case of heating from below is longitudinal.

In the case of heating from above ($M < 0$) an analytical investigation of the problem in the longwave limit gives the following leading order dispersion relation

$$(\Lambda^2 + GPk)\left(\Lambda^2 + \frac{|M|Pk^2}{1+P^{1/2}}\right) = 0. \tag{22}$$

Relation (22) determines two oscillatory modes, transverse (capillary-gravity) waves with frequency $\Omega_1 = \sqrt{GPk}$ and longitudinal (Marangoni) waves with the frequency

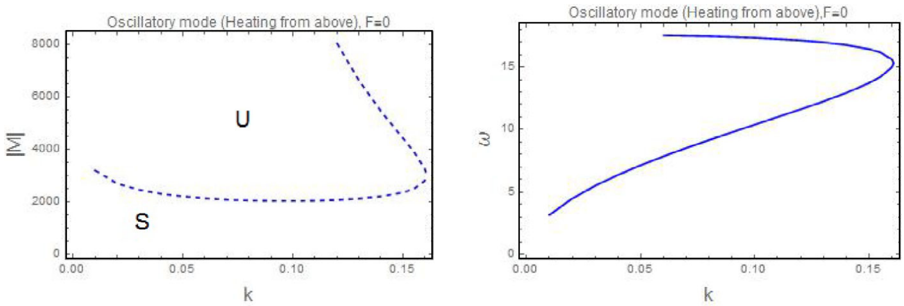

Fig. 3. Neutral curves for oscillatory instability modes and frequency of oscillations. Parameters: $G = 100$, $P = 10$, $N = 0.1$, and $L = 0.01$. Letters "S" and "U" indicate a stable and unstable regions, respectively.

$\Omega_2 = |M|^{1/2}P^{1/2}k/(1 + P^{1/2})^{1/2}$. Mixing of modes, which is observed in the next order of the asymptotic expansion, leads to an instability [10,11]. Numerical calculation of the complete dispersion relation gives us the neutral curve for oscillatory modes (Fig. 3a) and the frequency of oscillations (Fig. 3b). The instability region is bounded from below and from above. The lower boundary corresponds to the excitation of capillary-gravity waves, the upper boundary corresponds to the stabilization of Marangoni waves.

3.2 Oscillatory instabilities under parametric excitation

Here we consider the parametric excitation of the oscillatory modes described in the subsection above. Three types of response to the external parametric excitation are known. The first mode of instability is *harmonic*, where the response on external forcing occurs with frequency equal to the driving frequency. The second mode of the parametric instability is *subharmonic*, where the response has frequency equal to half of the driving frequency, and the third mode of the instability is *quasi-periodic*, when the frequency of response is not commensurate with the driving frequency.

It is necessary to distinguish between two qualitatively different cases. If there is no instability in the absence of vibration, i.e., the origin of the instability is solely the resonant parametric excitations of otherwise decaying waves, the instability in the presence of vibration is typically subharmonic or harmonic, while the quasi-periodic instability is either absent or irrelevant [6]. However, if the vibration acts on a system which has an intrinsic oscillatory instability in the absence of vibration, the situation is quite different. If the dependence of the frequency on the neutral curve in the absence of vibration is $\Omega(k)$, then neutral disturbances in the presence of vibration have the form of a Floquet function, i.e., they have nonzero Fourier components on the values of frequency $\Omega(k) \pm 2m\omega$, where m is integer. Because Ω and ω are typically incommensurate, one observes a quasiperiodic neutral curve which replaces the former oscillatory neutral curve. At the same time, for specific values of k satisfying the condition $\Omega(k) = n\omega$, where n is integer, the parametric resonance take place, which leads to the appearance of "bubbles" of subharmonic and harmonic instabilities attached to the quasiperiodic instability curve.

To find numerically the instability boundaries for harmonic and subharmonic modes we assume $\Lambda = 0$ in system (12)–(19) and decompose variables into the sets of harmonic functions as the Fourier expansions

$$\{w(z,t), \theta(z,t), \zeta(t), \gamma(t)\} = \sum_m \{w_m(z), \theta_m(z), \zeta_m, \gamma_m\}e^{im\omega t}. \tag{23}$$

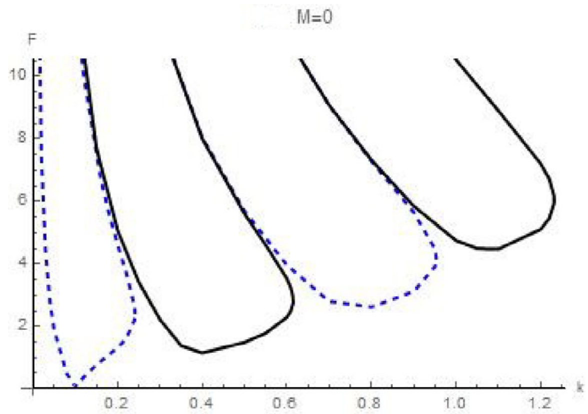

Fig. 4. Typical neutral curves. Dashed lines are boundaries for subharmonic regions, solid lines correspond to harmonic response. Parameters: $N = 0.1$, $L = 0.01$, $G = 100$, $P = 10$, $M = 0$.

Here $m = \pm 1, \pm 3, \ldots$ correspond to the subharmonic instability mode, and $m = 0, \pm 2, \pm 4, \ldots$ to the harmonic one. To find the quasi-periodic mode we apply Floquet theory. For that kind of instability $\Lambda = \Lambda_r + i\Lambda_i$ and on the stability boundary $\Lambda_r = 0$. The imaginary part Λ_i is defined modulo 2ω. Because the imaginary eigenvalues of the system (12)–(19) appear in pairs we can assume $0 \le \Lambda_i \le \omega$. Note that $\Lambda_i = 0$ corresponds to harmonic mode, $\Lambda_i = \omega$ corresponds to the subharmonic mode.

First, let us mention the case where the system is not heated, so there is no thermocapillary effect ($M = 0$). In this case, the typical neutral curves (parameter F as a function of wave number k), see Figure 4, are a set of alternately changing instability regions. The first region, closest to $k = 0$, is a subharmonic one, then follows a harmonic region, then again a subharmonic region, etc. This case is considered in detail in our paper [20].

3.2.1 Heating from above

Let us consider now heating from above. We fix the driving frequency at $2\omega = 20.8$ (in that case, the parametric excitation of waves is initiated near the minimum of the neutral stability curve found at $F = 0$) and begin increase the amplitude of the external forcing. As it is seen in Figure 5 the oscillatory mode is transformed to quasi-periodic (dashed line) and around that line a bubble of the subharmonic instability grows with increasing values of the parameter F (cf. [16]). This bubble appears at $k = 0.1$ at which the oscillatory frequency of the non-excited system exactly equals one-half the driving frequency of the external forcing ($\omega = 10.4$). At $F = 0.083$ the subharmonic bubble touches the line $M = 0$. With further increase of the parameter F, as seen from Figure 6, new subharmonic instability regions appear.

In the plane (F, k) we can see that for small heating (small values of $|M|$) the stability regions are similar to those in the case without heating (Fig. 4), but for greater values of $|M|$ the instability tongues overlap one another, see Figure 7b.

3.2.2 Heating from below

In the case of heating from below the oscillatory instability is characterized by smaller values of the frequency. For example, without external periodic forcing the threshold

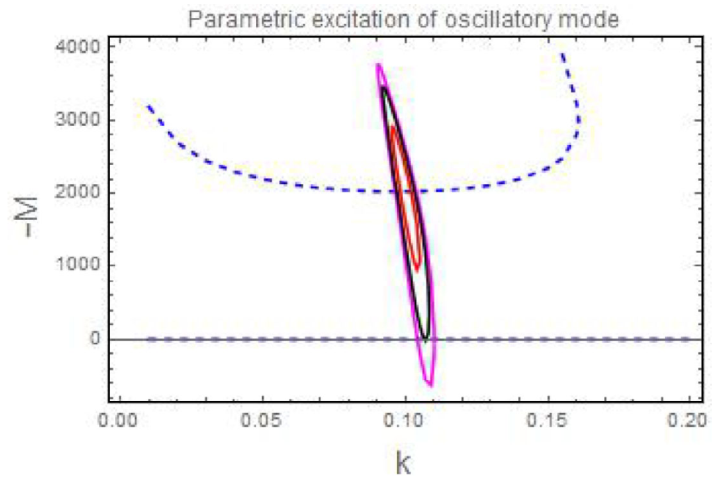

Fig. 5. Neutral stability curves for driving frequency $2\omega = 20.8$. Red color region is for $F = 0.05$, the magneta color region for $F = 0.1$, the black color bubble touches line $M = 0$ at $F = 0.083$.

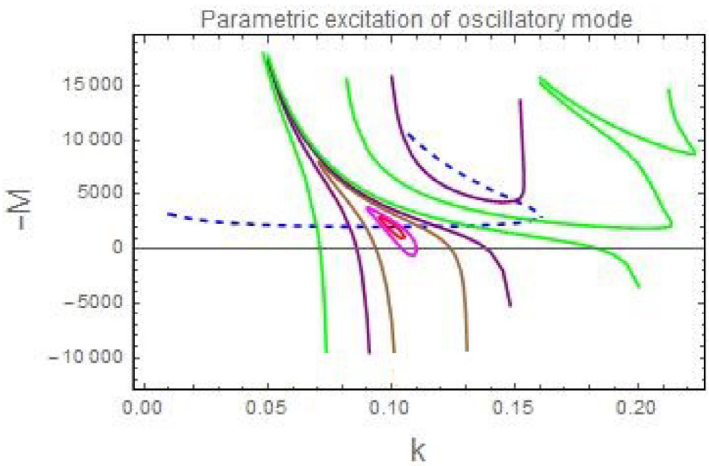

Fig. 6. Neutral stability curves for driving frequency $2\omega = 20.8$. Additional subharmonic regions: brown color region at $F = 0.3$, purple color region at $F = 0.5$ and green color region at $F = 1$. Dashed line – the oscillatory instability neutral curve for $F = 0$.

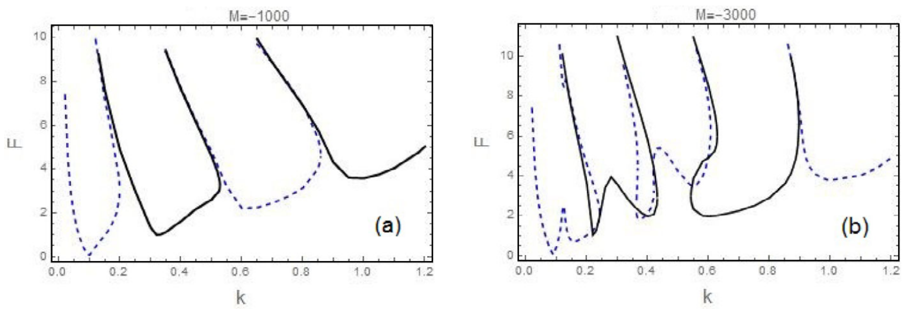

Fig. 7. Stability tongues, (F, k) plots. (a) $M = -1000$, (b) $M = -3000$. Parameters: $G = 100$, $P = 10$, $N = 0.1$, and $L = 0.01$.

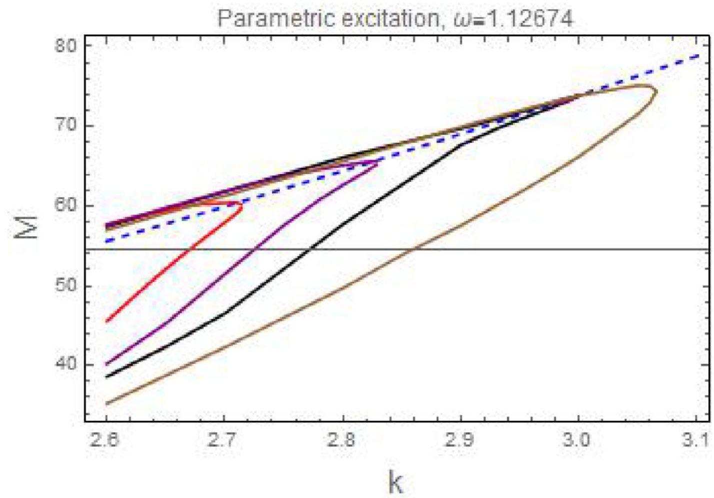

Fig. 8. Neutral stability curves for driving frequency $2\omega = 2.25348$. Subharmonic regions: red color region at $F = 9$, purple color region at $F = 9.5$, black color region at $F = 10$ and brown color region at $F = 12$. Dashed line – the oscillatory instability mode for non-excited situation.

value of the oscillatory instability at $k = 3$ equals $M_{osc} = 73.864$ and the oscillation frequency is $\omega = 1.12674$. Now, let us take the external forcing with driving frequency $2\omega = 2 \cdot 1.12674$ and growing value of the forcing amplitude. We can see that the neutral curve for the oscillatory mode is transformed to a quasi-periodic one. On this quasi-periodic instability line at wave number $k = 3$ corresponding to the driving frequency, a subharmonic bubble appears as in the previous case, but with increasing values of the parameter F this bubble does not grow as fast as in the case of heating from below. With further increase of the parameter F, this subharmonic bubble on the quasiperiodic line is merged with a bigger region of Faraday subharmonic instability.

Figure 8 shows a part of the neutral curves close to $k = 3$. The red color corresponds to a subharmonic region at $F = 9$, a purple color region is for $F = 9.5$, the black color is for $F = 10$ and the brown color region is for $F = 12$. The merging of this growing subharmonic region with the subharmonic bubble occurs at $F = 9.8$.

4 Conclusions

As shown in our previous works, different oscillatory modes can appear in a semi-infinite liquid volume covered by an insoluble surfactant, depending on heating conditions. If the system is heated from below then we have longitudinal dilational wave (*Marangoni wave*) on the free surface, but if the system is heated from above, then there exist two different types of possible waves on the free surface of the liquid: one is longitudinal and another one is transverse, or capillary-gravity, called also *Faraday waves.*

In this paper we consider the parametric excitation of these waves by periodic vertical vibration of the system. We find that periodic vibration can generate a set of alternately changing instability regions – subharmonic, harmonic, again subharmonic, etc. The most easily excited mode is the subharmonic one at the smallest values of the wave number. In the case of heating from above, at large values of the Marangoni number the subharmonic regions overlap with the harmonic ones. In the plots (M, k) we see that by heating from above at small values of fixed parameter F a subharmonic bubble appears and grows with increasing parameter F. For greater values of parameter F new subharmonic regions appear, and it makes the instability map very complex.

Another example is heating from below. There exist two subharmonic regions under the parametric excitation. The first one appears, as in the previous case, on the oscillatory neutral curve and looks like a bubble, but it does not significantly grow with increasing F. However, there exists also the second subharmonic zone corresponding to Faraday waves, which propagates fast along the oscillatory neutral curve and merges with the small subharmonic bubble.

AM was partially supported by the ERAU Research Award No.13373. The authors acknowledge unknown referees for their assistance in evaluating the manuscript.

References

1. M. Faraday, Phil. Trans. R. Soc. **121**, 299 (1831)
2. F. Melde, Ann. Phys. Chem. **109**, 193 (1859)
3. J.W. Strutt (Lord Rayleigh), Phil. Mag. **24**, 145 (1887)
4. L. Kühn, Jahr. für dracht. Teleg. und Telephone **9**, 502 (1915)
5. T.B. Benjamin, F. Ursell, Proc. R. Soc. Lond. A **225**, 505 (1954)
6. K. Kumar, Proc. R. Soc. Lond. A **452**, 1113 (1996)
7. G.Z. Gershuni, D.V. Lyubimov, *Thermal Vibrational Convection* (Wiley, Chichester, 1998)
8. G. Ahlers, P.C. Hohenberg, M. Lücke, Phys. Rev. A **32**, 3493 (1985)
9. B.L. Smorodin, A.B. Mikishev, A.A. Nepomnyashchy, B.I. Myznikova, Phys. Fluids **21**, 062102 (2009)
10. E.B. Levchenko, A.L. Chernyakov, Sov. Phys. JETP **54**, 102 (1981)
11. A.Ye. Rednikov, P. Colinet, M.G. Velarde, J.C. Legros, J. Non-Equilib. Thermodyn. **25**, 381 (2000)
12. A.A. Nepomnyashchy, M.G. Velarde, P. Colinet, *Interfacial Phenomena and Convection* (Chapman & Hall/CRC, Boca Raton, 2002)
13. J.C. Berg, A.A. Acrivos, Chem. Eng. Sci. **20**, 737 (1965)
14. H.J. Palmer, J.C. Berg, J. Fluid Mech. **51**, 385 (1972)
15. A.B. Mikishev, A.A. Nepomnyashchy, Microgravity Sci. Technol. **22**, 415 (2010)
16. A.B. Mikishev, A.A. Nepomnyashchy, Eur. Phys. J. Special Topics **219**, 81 (2013)
17. A.B. Mikishev, A.A. Nepomnyashchy, Eur. Phys. J. Special Topics **224**, 229 (2015)
18. H. Wong, C. Rumschitzki, C. Maldarelli, Phys. Fluids **8**, 3203 (1996)
19. A.B. Mikishev, A.A. Nepomnyashchy, Colloids Surf. A, DOI: `10.1016/j.colsurfa.2016.07.017` (2016)
20. A.B. Mikishev, B. Friedman, A.A. Nepomnyashchy, Fluid Dyn. Res. **48**, 061403 (2016)